Protein-Biomembrane interactions as therapeutic targets

*Marco M. Domingues, Pedro M. Matos, Filomena A. Carvalho, Nuno C. Santos**

Instituto de Medicina Molecular, Faculdade de Medicina da Universidade de Lisboa, Av. Prof. Egas Moniz, 1649-028 Lisboa, Portugal.

*** Corresponding author:** tel.: +351 217999480; fax: +351 217999477; e-mail: nsantos@fm.ul.pt

ABSTRACT

Biological membranes are dynamic structures essential for several cellular phenomena. The scope of the work of the Institute of Molecular Medicine (IMM) Biomembranes Unit is the study of biochemical and biophysical processes occurring at the membrane level on human cells and on their viral and bacterial pathogens. On the viral context, we are primarily interested on HIV and dengue virus, and particularly on the two steps of their life cycle involving their interaction with host cell membranes: the viral entry into target cells and the assembly of new viral particles. A special focus will be given to the study of the role of biological membranes on the mechanism of action of the HIV entry (membrane fusion) inhibitors enfuvirtide and T-1249. We are also involved in assessing the molecular basis of the activity of microbicides, such as $rBPI_{21}$, that bind to specific components of bacterial membranes. Additionally, our line of work on the binding of fibrinogen to erythrocytes, and its relevance as a cardiovascular risk factor will be presented. An approach to the latter problem by single-molecule force spectroscopy, using an atomic force microscope (AFM), allowed the molecular recognition, characterization and partial identification of the human erythrocyte receptor for fibrinogen.

1. FIBRINOGEN-ERYTHROCYTE MEMBRANE INTERACTION

Upon bleeding due to the opening of a wound on a blood vessel, the coagulation process is triggered. The plasma protein fibrinogen builds up the scaffold for the blood clot formation, by polymerizing in a fibrin network and entrapping the blood cells. The main physiological receptor for fibrinogen is the platelet membrane integrin $\alpha_{IIb}\beta_3$. As fibrinogen has more than one integrin-binding site, it is able to simultaneously bind two platelets, bridging them and regulating blood hemostasis.

Beside the relevance of the fibrinogen-platelet binding, it is also known that high plasma fibrinogen levels induce erythrocyte hyperaggregation [1-3], and that this increased aggregation constitutes a serious cardiovascular risk factor [4, 5]. This prompted us to study: (*i*) how does fibrinogen increase erythrocyte aggregation? (*ii*) Is there a specific receptor for fibrinogen on the erythrocyte membrane? (*iii*) Can this interaction be modulated to reduce hyperaggregation? These three questions were addressed by measuring fibrinogen-erythrocyte unbinding forces by atomic force microscopy (AFM) based force spectroscopy.For the sake of comparison the measurements of the fibrinogen-erythrocyte interaction were always conducted in parallel with measurements of the well known interaction of fibrinogen with platelets. It is worth of notice that the later interaction has been extensively studied, but not by the methodology described here.

AFM is mainly an imaging technique, in which the surface of a sample is scanned, line by line, by the movement of a thin tip, mounted on a flexible cantilever (for a review see, [6]). The tip-sample repulsion at the atomic level, transduced by the cantilever deflection and by an optical lever mechanism, permits the association of a height value to each position on the *x,y* plan and, therefore, the reconstitution of a pseudo-3D image of the sample surface. In addition to being used for imaging, the AFM can also be used to quantify the interaction between the tip and a specific spot of the sample, taking advantage of the pico-Newton sensitivity of the method. This

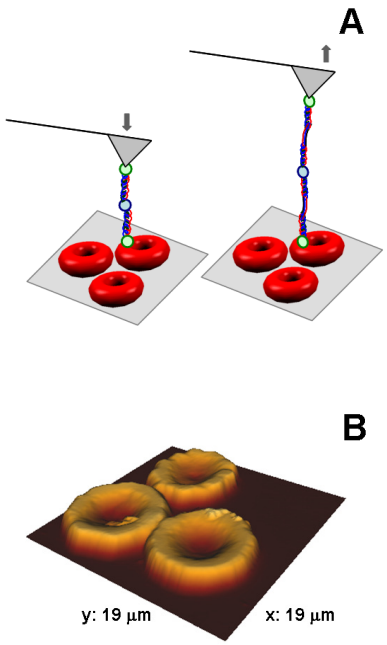

Figure 1: Force Spectroscopy technique at an Atomic Force Microscope. (A) Schematic representation of the erythrocytes deposited on a poly-L-lysine-coated glass slide and an AFM tip chemically functionalized with fibrinogen molecule(s). The arrows represent the approach and retraction cycles during the force spectroscopy measurements. When approaching the tip to the sample, the fibrinogen molecule may contact with cell receptor(s) and the binding between them can occur. By retracting the tip away from the sample, the binding force necessary to break this bond, at the single-molecule level, can be measured. (B) Air tapping-mode AFM images of typical circular, biconcave human erythrocytes, from healthy blood donors, deposited on poly-L-lysine coated glass slides (height 3D image). Reprinted from [10].

approach is usually termed "force spectroscopy" (despite not being in fact a "spectroscopy", as it is not based on the interaction of radiation with matter!).

On the context of this study, we used isolated human erythrocytes or platelets, in buffer, lightly adherent by electrostatic interactions to poly-L-lysine-treated glass slides. The force spectroscopy approach is based on the covalent attachment of fibrinogen molecules to the AFM silicon nitride tips, following methodologies previously applied to other proteins [7, 8]. After this, we use the AFM to tap with the fibrinogen-functionalized tip on the surface of the blood cell (Figure 1) [9, 10]. In the situations in which the binding occurs, the additional force necessary to detach the tip (and the fibrinogen molecule) from the cell can be calculated, based on force vs. distance curves [11]. After performing and analyzing hundreds or thousands of these binding / unbinding curves, a frequency *vs.* rupture force histogram can be built up. The fitting using Gaussian functions of the histogram peaks allowed the determination of the force necessary to break a single fibrinogen-cell interaction, with additional peaks corresponding to multiples of this value (Figure 2). The comparison of the results obtained by this methodology led us to a first surprise: The average force necessary to break the fibrinogen-erythrocyte interaction (79 ± 3 pN) is lower but quite comparable with the force necessary to break the fibrinogen-platelet interaction (97 ± 2 pN) [9], pointing out to the existence of a receptor for fibrinogen on the erythrocyte membrane, instead of the non-specific interaction previously proposed by some authors [3].

By performing identical measurements for different loading rates and analyzing the data with the Bell, Evans and Ritchie formalism [12-14], it was possible to obtain other parameters characterizing this interaction, namely, the energy and width of the energy barrier that must be overcome for the unbinding to occur, and the dissociation rate, or its inverse, the unperturbed bond lifetime. The results obtained for this last parameter allowed us to conclude that one of the reasons why the fibrinogen-erythrocyte binding is so difficult to study by more conventional methodologies, such as flow cytometry, is its reduced lifetime [9].

As it is common for integrins, the $\alpha_{IIb}\beta_3$ receptor for fibrinogen in platelets requires calcium to be functional. After the initial experiments, described above, being conducted in the presence of a physiological concentration of Ca^{2+}, new experiments were carried out in its absence, additionally adding EDTA to chelate any trace amount that could be present. As a first control or proof of concept to demonstrate that the interaction measured by force spectroscopy was in fact between fibrinogen and the blood cells membrane receptor, results obtained in the absence of Ca^{2+} demonstrate, as expected, the reduction of the fibrinogen-platelet binding, both in terms of force necessary to break the bond (decreasing to values characteristic of non-specific interactions) and of binding frequency [9]. The binding of fibrinogen to erythrocytes is also impaired by the absence of calcium. This observation suggested that the receptor for fibrinogen in erythrocytes is also an integrin.

As a second control, or proof of concept, we tested the effect of eptifibatide on the fibrinogen binding to either of the blood cells. This is a cyclic peptide derived from barbourin, a component of the venom of the southeastern pigmy rattlesnake [15]. It

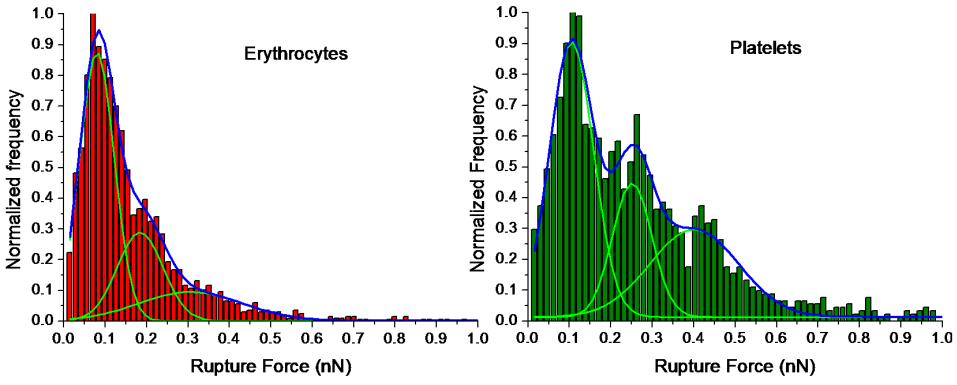

Figure 2: Force spectroscopy results from healthy human blood donors in the presence of Ca^{2+} 1 mM. Rupture-force histograms from about 8,000 single event-force measurements for the fibrinogen–erythrocyte (red) and fibrinogen-platelet (green) systems. Measurements were done with an applied force of 1 nN, pulling speed of 2 µm/s and at a loading rate of 4 nN/s. Reprinted with permission from [9] (© 2010, American Chemical Society).

is considered to be a specific inhibitor of the $\alpha_{IIb}\beta_3$ integrin, used in hospital settings to treat platelet hyperaggregation. As expected, eptifibatide inhibited fibrinogen-platelet binding at the extension and concentrations range expected based on the clinical studies [15, 16]. Regarding the binding to erythrocytes, eptifibatide also inhibited the binding of fibrinogen. However, the same threshold level of inhibition observed for platelets was reached only at higher eptifibatide concentrations [9]. This indicates that the receptor for fibrinogen on erythrocytes is not the glycoprotein $\alpha_{IIb}\beta_3$, but an $\alpha_{IIb}\beta_3$-related integrin.

All the results described so far were obtained using blood samples from healthy volunteer blood donors. As a third and final control or proof of concept, identical measurements were carried out with cells isolated from a blood sample of a patient with Glanzmann thrombasthenia. This is a rare hereditary disease which patients have impaired coagulation due to the absence of the $\alpha_{IIb}\beta_3$ receptor or its presence on a non-functional mutated form [17]. Expectedly, tapping with the fibrinogen-derivatized tip on platelets from this patient almost yielded no binding. On the few situations in which the binding occurred, the force necessary to break the bond was rather low, characteristic of non-specific interactions. Performing identical measurements with erythrocytes, we could demonstrate for the first time that Glanzmann thrombasthenia patients can also have impaired fibrinogen-erythrocyte binding [9]. Genetic studies were conducted to identify if the mutation responsible for the Glanzmann thrombasthenia in this patient was on the ITGA2B or on the ITGB3 gene (responsible for the expression of the α_{IIb} and β_3 sub-units of the platelet receptor, respectively). As the pathogenic mutation was identified on the ITGB3 gene, we could demonstrate that one of the two sub-units of the receptor for fibrinogen on the erythrocyte membrane is a product of the expression of this gene. New experiments are being conducted to identify the other sub-unit of the receptor.

In parallel, we also evaluated the effect of erythrocyte aging on the ability to bind fibrinogen [10]. The results indicated that upon erythrocytes aging, there was a significant decrease on the fibrinogen binding, by decreasing the frequency of its occurrence but not its binding strength. For the binding between fibrinogen and erythrocytes to occur, a lower fibrinogen concentration was needed on young erythrocytes than for the older ones. We could conclude that the fibrinogen-erythrocyte receptor binding can be lost, masked or progressively turned to non-functional with the *in vivo* erythrocyte senescence process. Knowing that younger erythrocytes bind more to fibrinogen, we could presume that this population is the main responsible for some cardiovascular diseases associated with an increase on the fibrinogen content in blood, which could disturb its normal flow.

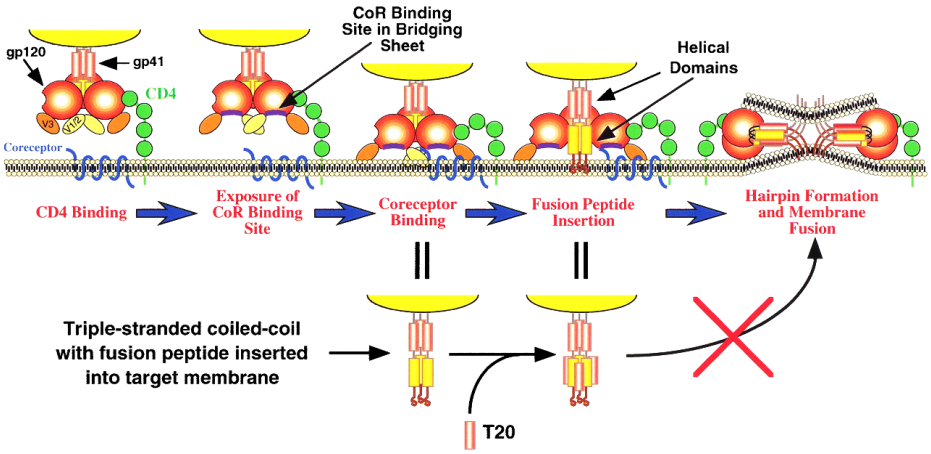

Figure 3: Steps required for HIV-1 glycoprotein mediated membrane fusion with the host cells, as explained in the main text. A fusion inhibitor peptide (e.g., enfuvirtide and T-1249) may block the formation of the six-helix bundle, preventing the fusion of the viral and cell membranes. Reprinted with permission from [45] (© 2000, Cold Spring Harbor Laboratory Press).

2. HIV FUSION INHIBITORS

The infection of a target cell by the human immunodeficiency virus type 1 (HIV-1) is mediated by the gp120-gp41 viral glycoproteins complex (a homotrimer of heterodimers). gp120 binds to the cell receptor CD4 and to a co-receptor, usually CCR5 or CXCR4 [18]. After these bindings, gp41 is exposed, acquiring an extended conformation and enabling the insertion of its fusion peptide in the target cell membrane. Subsequently, another conformational change takes place, in which two heptad repeat domains of each of the three gp41 monomers come together, forming a structure named six-helix bundle. It brings the viral and cell membranes together, enabling the formation of the fusion pore and the entrance of the viral content into the cell [19] (Figure 3).

HIV fusion inhibitor peptides were initially designed with a sequence corresponding to one of the heptad repeat domains, in order to inhibit the binding to the opposite heptad repeat domain of gp41, impairing the six-helix bundle formation and, therefore, the entry of the viral content into the target cell [20]. Experimental evidences showed that this is, at least, a partial explanation, as inhibitors with a higher binding to the gp41 heptad repeat domain were shown to be ineffective *in vivo*, while some peptides with a lower binding to gp41 are efficient [21].

The peptides enfuvirtide (T-20) and T-1249 are two of these HIV fusion inhibitors. Enfuvirtide is the only fusion inhibitor approved so far for clinical use. Its sequence corresponds to part of the HIV gp41 C-terminal

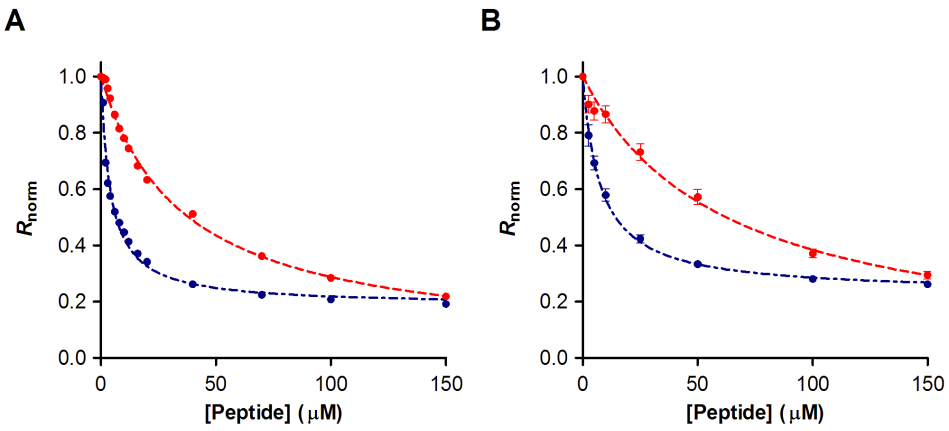

Figure 4: Peptide affinity towards erythrocytes and PBMC cell membranes. The plots represent the dependence of the ratio on the enfuvirtide (red) and T-1249 (blue) concentrations for erythrocytes (A) and PBMC (B), the dashed curves are fittings to a single binding site model. Ratio values were normalized for the initial value of zero peptide concentration. Plotted values represent the mean ± standard error of mean (error bars not visible for erythrocytes due to small errors). N = 6 for erythrocytes and N = 7 for PBMC. Reprinted from [24].

heptad repeat domain. T-1249 is a second generation drug, with successful preliminary clinical results, which development is presently on hold. Its sequence includes elements from fusion proteins of HIV-1, HIV-2 and SIV (simian immunodeficiency virus). In a line of work developed together with Miguel Castanho's group (formerly at the Faculty of Sciences of the University of Lisbon, and now also at the Institute of Molecular Medicine (IMM) / Faculty of Medicine of the University of Lisbon), we have used the intrinsic fluorescence of the tryptophan residues in both peptides to study their interaction with biomembrane model systems (lipid vesicles) [22, 23]. In these studies, we showed that enfuvirtide and T-1249 partition to fluid phase lipid membranes, and that T-1249 (but not enfuvirtide) additionally adsorbs to the surface of cholesterol rich membrane domains.

Recently, we extend these observations to the interaction of enfuvirtide and T-1249 with biological membranes, using human PBMC (peripheral blood mononuclear cells) and erythrocytes [24]. PBMC were chosen because they include one of the main targets for HIV infection: $CD4^+$ T-lymphocytes. Erythrocytes are not infected by HIV. However, it is found *in vivo* bound to the erythrocyte membrane, constituting a significant reservoir of infective viruses, even during highly active antiretroviral therapy (HAART) [25, 26].

To study the interaction of the peptides with the cell membranes, we could not use the same methodology as on the previous studies with biomembrane model systems (changes on peptide fluorescence properties upon membrane insertion [27]), as the fluorescence of the peptides would be masked by the fluorescence of the innumerous aromatic amino acid residues of the different protein components of the cells. Therefore, a new strategy had to be used: Instead of looking at the fluorescence of the peptide itself, we followed the changes induced by the peptide on the fluorescence of a membrane probe sensitive to the membrane potential [28]. After testing different fluorescent probes, we choose to use di-8-ANEPPS (4-[2-[6-(dioctylamino)-2-naphthalenyl] ethenyl]-1-(3-sulfopropyl)-pyridinium) for that purpose. The fluorescence of di-8-ANEPPS is highly sensitive to the membrane dipole potential, with an increase on this potential leading to a blue-shift on the probe excitation spectra. Quantitatively, the variations of the membrane dipole potential are easier to assess using as experimental output the ratio between the values obtained at two wavelengths of the fluorescence difference spectrum (obtained subtracting the spectrum without peptide from the spectrum obtained for a given concentration of the peptide).

di-8-ANEPPS was shown by confocal microscopy to properly label the cell membranes of PBMC and erythrocytes [24]. By adding enfuvirtide or T-1249 to the labeled cells, the shape of the difference spectra revealed concentration-dependent shifts to the red, indicative of a decrease in membrane dipole potential upon the binding of these peptides. The quantitative values allowed the calculation of the peptide-cell dissociation constants [24]. This way, both peptides were shown to interact with erythrocyte and lymphocyte membranes. There is a complete agreement between these results and the data previously obtained with biomembrane model systems [22, 23]. T-1249 has an affinity for these blood cells approximately eight-fold higher than enfuvirtide (Figure 4). This can be related with its higher partition constant and with the ability to adsorb to cholesterol-rich membrane domains, probably contributing for its improved antiretroviral efficacy [22].

In order to close the gap between the results obtained with biomembrane model systems, using the peptides intrinsic tryptophan fluorescence, and those obtained with blood cells, based on di-8-ANEPPS fluorescence, we also performed experiments using di-8-ANEPPS-labelled lipid vesicles, with different membrane compositions. The results were in agreement with the expected, with the addition of cholesterol to fluid phase lipid vesicles leading to a decrease on the enfuvirtide-membrane binding and to an increase on the binding of T-1249 [24].

Based on our findings, we proposed a model in which the HIV-1 association with erythrocytes *in vivo* could constitute a route to deliver peptide to the viral membranes (Figure 5). This should be especially rel-

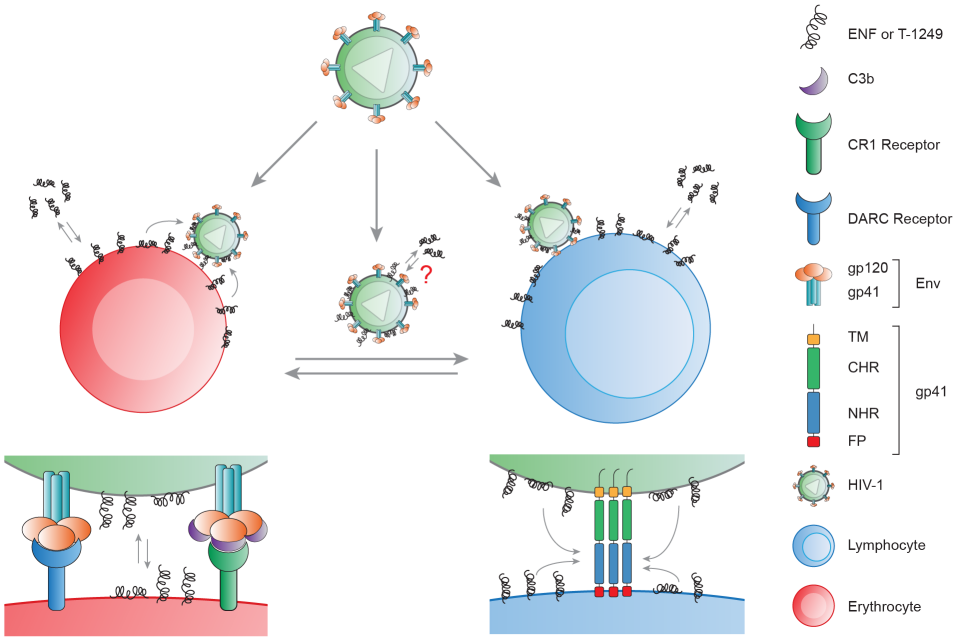

Figure 5: Proposed mode of action of enfuvirtide and T-1249 in circulation with blood cells. Reprinted from [24].

evant for T-1249, as the viral membrane is rich in cholesterol [29]. Regarding lymphocytes, their membrane can concentrate and accelerate the drug interactions with its molecular target, gp41 in its exposed conformation. The local enrichment of the inhibitor at the membrane level would increase the probability of taking advantage of the narrow spatial and time window during which gp41 is in the extended conformation in order to bind to it.

Going against the "textbook dogma" that the membrane fusion step of HIV-1 infection occurs at the surface of the cell, the group of Gregory Melikian published in 2009 a study with compelling evidences for an entry of HIV-1 via endocytosis [30]. Subsequent evidences additionally supported this theory [31]. If this is true, the relevance of the membrane binding of HIV fusion inhibitors is further strengthened, as a possible endocytic entry pathway would protect HIV from a fusion inhibitor only present in solution. However, its membrane binding and enrichment would drastically increase the inhibitory efficacy, by assuring a significant concentration to be present at the endosome level, where membrane fusion would occur.

Recently, the same experimental approach was also used for sifuvirtide, another second generation HIV fusion inhibitor that successfully completed phase IIb clinical trials in 2010 [32].

3. $rBPI_{21}$ MOLECULAR LEVEL MECHANISM OF ACTION

Section 1 was dedicated to an AFM-based force microscopy approach to a specific subject. Section 2 describes the use of fluorescence spectroscopy to address another one. Finally, in Section 3 another line of work ongoing at the Biomembranes Unit of IMM will be described; namely, the study of the mechanism of action of the antimicrobial protein $rBPI_{21}$, addressed by a different methodology: light scattering spectroscopy.

Gram-negative bacteria have two membranes, separated by a peptidoglycan layer. The outer leaflet of their outer membrane is constituted mainly of lipopolysaccharide (LPS). Both the inner membrane and the inner leaflet of the outer membrane do not present LPS, having in their content high proportions of negative phospholipids, such as phosphatidylglycerol (PG). LPS is also negatively charged. Upon infection by Gram-negative bacteria, it is the causative agent of sepsis. At high concentrations, LPS may lead to septic shock and, eventually, to death [33].

Our organism has two structurally similar proteins that bind LPS: the LPS-binding protein (LBP) and the bactericidal/permeability-increasing protein (BPI). Despite the structural similarity, their binding to LPS leads to opposite outcomes: The binding of LBP to LPS enables the activation of the inflammatory cascade, through the binding to CD14 [34]. On the contrary, the binding of BPI to LPS allows its neutralization and clearance, together with the blocking of the inflammatory cascade [34].

BPI is produced by neutrophils. It exerts its antibacterial activity both intracellularly (at the azurophil or primary granules of the neutrophil) and extracellularly (release of antimicrobial peptides and proteins from the specific or secondary granules during neutrophil activation). This protein has a boomerang-like shape, with a cationic N-terminal domain, responsible for the antimicrobial activity and LPS neutralization, and with the C-terminal being responsible for cell-recognition [35, 36]. $rBPI_{21}$ was designed with the sequence of the 193 amino acid residues of the N-terminal of BPI, except for the change of a cysteine for an alanine [37].

To study the mechanism of action of $rBPI_{21}$, we used mainly dynamic light scattering (DLS) and zeta-potential measurements [38, 39]. DLS spectroscopy is based on the evaluation of the Brownian motion of the scattering particle, in order to obtain its diffusion coefficient and, based on it, to calculate the hydrodynamic radius or diameter of the particle using the Stokes-Einstein equation. Zeta-potential is a parameter that can be used to evaluate the electrostatic interaction between particles and

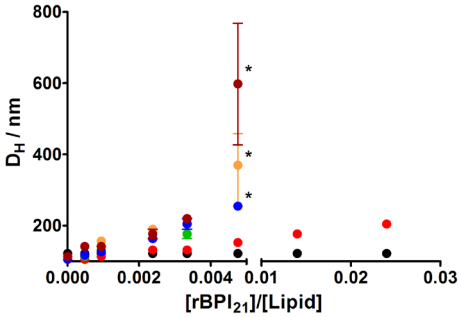

Figure 6: Aggregation of LUV caused by $rBPI_{21}$. Hydrodynamic diameter variation of lipid vesicles with increasing $rBPI_{21}$ concentration. Bars represents the size range from three independent experiments. Larger ranges are intrinsically associated to vesicles flocculation/precipitation (marked *). POPC (black); POPG (blue); POPC:POPG 55:45 (orange); POPC:POPG 80:20 (green); POPC:LPS 80:20 (red); POPC:POPG:LPS 60:20:20 (brown). Reprinted from [40].

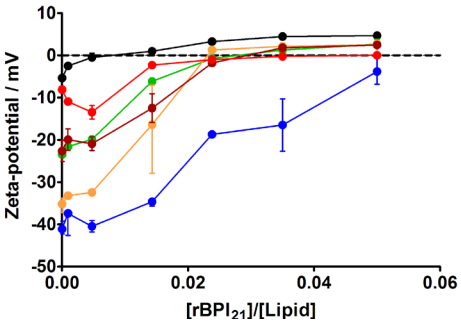

Figure 7: Zeta-potential for membrane model systems in the presence of $rBPI_{21}$. Bars represent the zeta-potential range from at least two independent experiments. POPC (black); POPG (blue); POPC:POPG 55:45 (orange); POPC:POPG 80:20 (green); POPC:LPS 80:20 (red); POPC:POPG:LPS 60:20:20 (brown). The lipid concentration was kept constant at 200 μM. Reprinted from [40].

to give information on the stability of colloidal dispersions. Most of the particles in aqueous solution carry an electric charge and this charge influences the distribution of the ions at the particle surface. The counterions attached to the particle create an electrical double layer, with an inner region (Stern layer), where the ions are firmly attached, and an outer layer, where the ions diffuse more freely. In this diffuse layer, there is a boundary where ions and particle inside it form a stable entity. During the zeta-potential measurements, an electric field is superimposed to the random Brownian motion. When a scattering particle is moving, ions within the boundary region move with the particle. The zeta-potential is defined as the potential created at this boundary [38].

In this study, we started by following the changes on the size and zeta-potential of the LPS aggregates naturally formed in solution [40]. Upon their titration with $rBPI_{21}$, there was a marked increase of the hydrodynamic diameter of the aggregates, with the size distribution becoming bimodal above a threshold level of the [$rBPI_{21}$]/[LPS] ratio. The zeta-potential of the LPS aggregates (in the absence of $rBPI_{21}$) is highly negative. With the addition of $rBPI_{21}$, it progressively increases, leveling up at positive zeta-potential values.

The interaction of $rBPI_{21}$ with biomembrane model systems (large unilamellar vesicles; LUV) with different lipid compositions was also addressed [40, 41], including systems containing LPS and/or POPG (palmitoyloleoylphosphatidylglycerol), in order to mimetize Gram-negative bacteria membranes. On previous studies, we participated on the development of spectroscopical methodologies to quantify the partition constant (K_p) of a given molecule between the aqueous phase and membranes (for reviews see, [27, 42, 43]). Based on the changes on the intrinsic fluorescence of the tryptophan residues of $rBPI_{21}$ upon membrane binding (followed by fluorescence spectroscopy), we measured its partition to membranes of different lipid compositions, and verified that high partitions to membranes occurred not only to LPS-containing systems, but also to membranes containing negative phospholipids, such as POPG [41]. By the opposite, no significant partition was observed for LUV made exclusively of zwitterionic (neutral) phospholipids, such as POPC (palmitoyloleoylphosphatidylcholine). By using DLS to assess the lipid vesicles size variations induced by the presence of increasing concentrations of $rBPI_{21}$, we realized that extensive aggregation was induced in the presence of POPG in the membranes, but not by the presence of LPS or POPC (Figure 6) [40]. Zeta-potential measurements shown that there is a higher affinity of $rBPI_{21}$ for POPC:POPG mixtures, relative to pure POPG (Figure 7). Therefore, the $rBPI_{21}$ interaction with membranes is not purely electrostatic.

To complement the DLS and zeta-potential studies, two other types of measurements were conducted, namely, membrane fusion and membrane leakage assays, in order to evaluate if these processes are promoted by $rBPI_{21}$ [40]. For the membrane fusion (lipid mixing) assay, we used a Förster resonance energy transfer (FRET; see Fernandes *et al.* in this Canal BQ issue) methodology, with nitro-2-1,3-benzoxadiazol-4-yl-dipalmitoylphosphatidylehtanolamine (NBD-PE) as donor and sulforhodamine B-dipalmitoylphosphatidylehtanolamine (RhB-PE) as acceptor. One-fourth of the LUV used for the assay was labeled with both fluorescent membrane probes, while the remaining lipid vesicles were unlabeled. The fusion efficiency could be calculated based on the decrease of the energy transfer between both probes, as the fusion between labeled and unlabeled vesicles increases the average distance between the two probes (surface dilution effect). With this assay, we observed that the $rBPI_{21}$-induced membrane fusion (tested with increasing concentrations of the protein) is promoted by the presence of POPG, but not by the presence of LPS or POPC.

For the membrane leakage assay, we used LUV with carboxyfluorescein entrapped on their lumen. This fluorescent probe, when at high concentrations, undergoes a fluorescence self-quenching effect. Thus, the quantification is made by adding the protein and registering the eventual increase of the carboxyfluorescein fluorescence due to its dilution upon leakage. In order to obtain a reference value, total leakage was promoted afterwards by adding triton X-100. The results showed that $rBPI_{21}$ promotes membrane leakage as long as the lipid membrane contains either POPG or LPS.

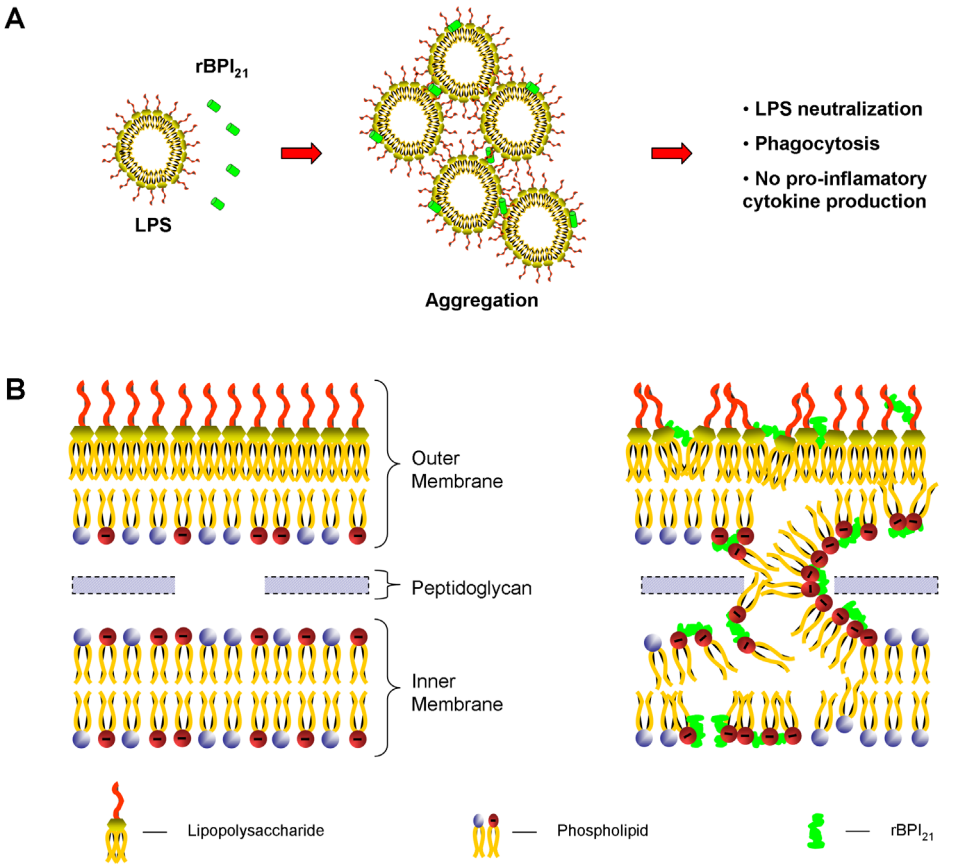

Figure 8: Schematic representation of the proposed mechanism of action of $rBPI_{21}$. (A) The protein interacts with LPS aggregates promoting their aggregation, which allow LPS phagocytosis by innate immune cells and reduce LPS availability for its receptor. (B) $rBPI_{21}$ interacts electrostatically with the LPS of the outer leaflet of outer membrane. This interaction disrupts the higher tight bond of the LPS, which allow the peptide insertion and translocation to the outer membrane inner leaflet and to the intermembrane space. $rBPI_{21}$ induces the fusion (or hemifusion) of the inner leaflet of the outer membrane and the inner membrane (both rich in PG). These membrane fusion events increase the membrane permeability, culminating with the leakage of the bacterial content. Reprinted from [40].

Based on these and on other complementary results, we proposed a model to explain the molecular basis of the $rBPI_{21}$ effects [40]: The interaction of this protein with the LPS aggregates in solution causes their massive aggregation. This process may impair the recognition by LPS receptors, and facilitate the phagocytosis of the aggregates by macrophages. Regarding the interaction with membranes, it is highly dependent on their composition. $rBPI_{21}$ can partition to the outer membrane of Gram-negative bacteria (rich in LPS and PG), attain an equilibrium with the intermembrane space, and reach the inner membrane. As both the inner leaflet of the outer membrane and the inner membrane are rich in PG, $rBPI_{21}$ may promote the fusion (or hemifusion) of the two bacterial membranes (Figure 8). This can create a leakage or, at lower concentrations, an increased permeability across the membranes, leading to cell death. This increased permeability had already been previously reported [44]. Based on our findings, the disruption of mammalian membranes by $rBPI_{21}$ is prevented by the absence of LPS and by the low content of POPG.

Calorimetry and atomic force microscopy experiments are being conducted in order to complement the previous findings.

OTHER PROJECTS

Adding to the lines of work addressed in the present article, the IMM Biomembranes Unit is also involved on the study of some poorly understood steps of the dengue virus life cycle, and on the identification of the mechanism of action at the molecular level of another family of antimicrobial peptides (AMP) and cell-penetrating peptides (CPP).

ACKNOWLEDGMENTS

The study described in Section 1 of this article counted with the valuable collaborations of Simon Connell (School of Physics, University of Leeds, UK), Robert Ariëns (Unit of Molecular Vascular Medicine, University of Leeds, UK), Alice Tavares (Hospital de Santa Maria – Centro Hospitalar de Lisboa Norte) and Gabriel Miltenberger-Miltenyi (GenoMed, Lisbon). The projects of Sections 2 and 3 were developed together with Miguel Castanho (IMM / FMUL) and his group.

These lines of work were supported by Fundação para a Ciência e a Tecnologia – Ministério da Ciência, Tecnologia e Ensino Superior (FCT-MCTES, Portugal; projects PTDC/SAU-OSM/73449/2006 and PTDC/QUI-BIQ/104787/2008), by the FP7-PEOPLE IRSES (International Research Staff Exchange Scheme) project MEMPEPACROSS (EU), and by Fundação Calouste Gulbenkian (Portugal). MMD and PMM also thank FCT-MCTES for the PhD fellowships SFRH/BD/41750/2007 and SFRH/BD/42205/2007, respectively.

REFERENCES

1. Kwaan HC (2010) Role of plasma proteins in whole blood viscosity: a brief clinical review. *Clin Hemorheol Microcirc* **44**, 167-176.

2. Lominadze D, Schuschke DA, Joshua IG & Dean WL (2002) Increased ability of erythrocytes to aggregate in spontaneously hypertensive rats. *Clin Exp Hypertens* **24**, 397-406.

3. Maeda N, Seike M, Kume S, Takaku T & Shiga T (1987) Fibrinogen-induced erythrocyte aggregation: erythrocyte-binding site in the fibrinogen molecule. *Biochim Biophys Acta* **904**, 81-91.

4. Delamaire M & Durand F (1990) Erythrocyte aggregation and vascular pathology. *J Mal Vasc* **15**, 344-345.

5. Falco C, Vaya A, Simo M, Contreras T, Santaolaria M & Aznar J (2005) Influence of fibrinogen levels on erythrocyte aggregation determined with the Myrenne aggregometer and the Sefam erythro-aggregometer. *Clin Hemorheol Microcirc* **33**, 145-151.

6. Santos NC & Castanho MA (2004) An overview of the

biophysical applications of atomic force microscopy. *Biophys Chem* **107**, 133-149.

7. de Odrowaz Piramowicz M, Czuba P, Targosz M, Burda K & Szymonski M (2006) Dynamic force measurements of avidin-biotin and streptavdin-biotin interactions using AFM. *Acta Biochim Pol* **53**, 93-100.

8. Barattin R & Voyer N (2008) Chemical modifications of AFM tips for the study of molecular recognition events. *Chem Commun (Camb)*, 1513-1532.

9. Carvalho FA, Connell S, Miltenberger-Miltenyi G, Pereira SV, Tavares A, Ariens RA & Santos NC (2010) Atomic force microscopy-based molecular recognition of a fibrinogen receptor on human erythrocytes. *ACS Nano* **4**, 4609-4620.

10. Carvalho FA, de Oliveira S, Freitas T, Goncalves S & Santos NC (2011) Variations on fibrinogen-erythrocyte interactions during cell aging. *PLoS One* **6**, e18167.

11. Heinz WF & Hoh JH (1999) Spatially resolved force spectroscopy of biological surfaces using the atomic force microscope. *Trends Biotechnol* **17**, 143-150.

12. Bell GI (1978) Models for the specific adhesion of cells to cells. *Science* **200**, 618-627.

13. Evans E & Ritchie K (1997) Dynamic strength of molecular adhesion bonds. *Biophys J* **72**, 1541-1555.

14. Lee CK, Wang YM, Huang LS & Lin S (2007) Atomic force microscopy: determination of unbinding force, off rate and energy barrier for protein-ligand interaction. *Micron* **38**, 446-461.

15. Holmes MB, Sobel BE & Schneider DJ (1999) Variable responses to inhibition of fibrinogen binding induced by tirofiban and eptifibatide in blood from healthy subjects. *Am J Cardiol* **84**, 203-207.

16. Katori N, Szlam F, Levy JH & Tanaka KA (2004) A novel method to assess platelet inhibition by eptifibatide with thrombelastograph. *Anesth Analg* **99**, 1794-1799.

17. Nurden AT (2006) Glanzmann thrombasthenia. *Orphanet J Rare Dis* **1**, 10-17.

18. Wyatt R & Sodroski J (1998) The HIV-1 envelope glycoproteins: fusogens, antigens, and immunogens. *Science* **280**, 1884-1888.

19. Chan DC & Kim PS (1998) HIV entry and its inhibition. *Cell* **93**, 681-684.

20. Wild CT, Shugars DC, Greenwell TK, McDanal CB & Matthews TJ (1994) Peptides corresponding to a predictive alpha-helical domain of human immunodeficiency virus type 1 gp41 are potent inhibitors of virus infection. *Proc Natl Acad Sci U S A* **91**, 9770-9774.

21. Liu S, Lu H, Niu J, Xu Y, Wu S & Jiang S (2005) Different from the HIV fusion inhibitor C34, the anti-HIV drug Fuzeon (T-20) inhibits HIV-1 entry by targeting multiple sites in gp41 and gp120. *J Biol Chem* **280**, 11259-11273.

22. Veiga AS, Santos NC, Loura LM, Fedorov A & Castanho MA (2004) HIV fusion inhibitor peptide T-1249 is able to insert or adsorb to lipidic bilayers. Putative correlation with improved efficiency. *J Am Chem Soc* **126**, 14758-14763.

23. Veiga S, Henriques S, Santos NC & Castanho M (2004) Putative role of membranes in the HIV fusion inhibitor enfuvirtide mode of action at the molecular level. *Biochem J* **377**, 107-110.

24. Matos PM, Castanho MA & Santos NC (2010) HIV-1 fusion inhibitor peptides enfuvirtide and T-1249 interact with erythrocyte and lymphocyte membranes. *PLoS One* **5**, e9830.

25. Hess C, Klimkait T, Schlapbach L, Del Zenero V, Sadallah S, Horakova E, Balestra G, Werder V, Schaefer C, Battegay M & Schifferli JA (2002) Association of a pool of HIV-1 with erythrocytes in vivo: a cohort study. *Lancet* **359**, 2230-2234.

26. Beck Z, Brown BK, Wieczorek L, Peachman KK, Matyas GR, Polonis VR, Rao M & Alving CR (2009) Human erythrocytes selectively bind and enrich infectious HIV-1 virions. *PLoS One* **4**, e8297.

27. Santos NC, Prieto M & Castanho MA (2003) Quantifying molecular partition into model systems of biomembranes: an emphasis on optical spectroscopic methods. *Biochim Biophys Acta* **1612**, 123-135.

28. Matos PM, Goncalves S & Santos NC (2008) Interaction of peptides with biomembranes assessed by potential-sensitive fluorescent probes. *J Pept Sci* **14**, 407-415.

29. Brugger B, Glass B, Haberkant P, Leibrecht I, Wieland FT & Krausslich HG (2006) The HIV lipidome: a raft with an unusual composition. *Proc Natl Acad Sci U S A* **103**, 2641-2646.

30. Miyauchi K, Kim Y, Latinovic O, Morozov V & Melikyan GB (2009) HIV enters cells via endocytosis and dynamin-dependent fusion with endosomes. *Cell* **137**, 433-444.

31. Miyauchi K, Marin M & Melikyan GB (2011) Visualization of retrovirus uptake and delivery into acidic endosomes. *Biochem J* **434**, 559-569.

32. Matos PM, Freitas T, Castanho MA & Santos NC (2010) The role of blood cell membrane lipids on the mode of action of HIV-1 fusion inhibitor sifuvirtide. *Biochem Biophys Res Commun* **403**, 270-274.

33. Raetz CR & Whitfield C (2002) Lipopolysaccharide endotoxins. *Annu Rev Biochem* **71**, 635-700.

34. Weiss J (2003) Bactericidal/permeability-increasing protein (BPI) and lipopolysaccharide-binding protein (LBP): structure, function and regulation in host defence against Gram-negative bacteria. *Biochem Soc Trans* **31**, 785-790.

35. Beamer LJ, Carroll SF & Eisenberg D (1997) Crystal structure of human BPI and two bound phospholipids at 2.4 angstrom resolution. *Science* **276**, 1861-1864.

36. Beamer LJ, Carroll SF & Eisenberg D (1998) The BPI/LBP family of proteins: a structural analysis of conserved regions. *Protein Sci* **7**, 906-914.

37. Horwitz AH, Carroll SF, Williams RE & Liu PS (2000) Inclusion of S-sepharose beads in the culture medium significantly improves recovery of secreted rBPI(21) from transfected CHO-K1 cells. *Protein Expr Purif* **18**, 77-85.

38. Domingues MM, Santiago PS, Castanho MA & Santos NC (2008) What can light scattering spectroscopy do for membrane-active peptide studies? J Pept Sci 14, 394-400.

39. Santos NC & Castanho MA (1996) Teaching light scattering spectroscopy: the dimension and shape of tobacco mosaic virus. *Biophys J* **71**, 1641-1650.

40. Domingues MM, Castanho MA & Santos NC (2009) $rBPI_{21}$ promotes lipopolysaccharide aggregation and exerts its antimicrobial effects by (hemi)fusion of PG-containing membranes. *PLoS One* **4**, e8385.

41. Domingues MM, Lopes SC, Santos NC, Quintas A & Castanho MA (2009) Fold-unfold transitions in the selectivity and mechanism of action of the N-terminal fragment of the bactericidal/permeability-increasing protein ($rBPI_{21}$). *Biophys J* **96**, 987-996.

42. Matos PM, Franquelim HG, Castanho MA & Santos NC (2010) Quantitative assessment of peptide-lipid interactions. Ubiquitous fluorescence methodologies. *Biochim Biophys Acta* **1798**, 1999-2012.

43. Ribeiro MM, Melo MN, Serrano ID, Santos NC & Castanho MA (2010) Drug-lipid interaction evaluation: why a 19th century solution? *Trends Pharmacol Sci* **31**, 449-454.

44. Wiese A, Brandenburg K, Carroll SF, Rietschel ET & Seydel U (1997) Mechanisms of action of bactericidal/permeability-increasing protein BPI on reconstituted outer membranes of gram-negative bacteria. *Biochemistry* **36**, 10311-10319.

45. Doms RW & Trono D (2000) The plasma membrane as a combat zone in the HIV battlefield. *Genes Dev* **14**, 2677-2688.